การศึกษาผลของกลูตารอลดีไฮด์อิริโทรพอยอิตินต่อการเปลี่ยนแปลงของเซลล์ไต HEK293 ที่ได้รับอนุภาคเงินระดับนาโนเมตร

นางสาวขนิษฐา สุขเลิศ

วิทยานิพนธ์นี้เป็นส่วนหนึ่งของการศึกษาตามหลักสูตรปริญญาวิทยาศาสตรดุษฎีบัณฑิต
สาขาวิชาชีวเวชศาสตร์ (สหสาขาวิชา)
บัณฑิตวิทยาลัย จุฬาลงกรณ์มหาวิทยาลัย
ปีการศึกษา 2558

STUDY OF CYTOPROTECTIVE EFFECT OF GLUTARALDEHYDE ERYTHROPOIETIN ON HEK293 KIDNEY CELL AFTER SILVER NANOPARTICLE EXPOSURE.

Miss Kanidta Sooklert

A Dissertation Submitted in Partial Fulfillment of the Requirements
for the Degree of Doctor of Philosophy Program in Biomedical Sciences
(Interdisciplinary Program)
Graduate School
Chulalongkorn University
Academic Year 2015

Thesis Title	STUDY OF CYTOPROTECTIVE EFFECT OF GLUTARALDEHYDE ERYTHROPOIETIN ON HEK293 KIDNEY CELL AFTER SILVER NANOPARTICLE EXPOSURE.
By	Miss Kanidta Sooklert
Field of Study	Biomedical Sciences
Thesis Advisor	Assistant Professor Amornpun Sereemaspun, M.D., Ph.D.
Thesis Co-Advisor	Krissanapong Manotham, M.D.

Accepted by the Graduate School, Chulalongkorn University in Partial Fulfillment of the Requirements for the Doctoral Degree

.....Dean of the Graduate School
(Associate Professor Sunait Chutintaranond, Ph.D.)

THESIS COMMITTEE

.....Chairman
(Professor Shanop Shuangshoti, M.D.)
.....Thesis Advisor
(Assistant Professor Amornpun Sereemaspun, M.D., Ph.D.)
.....Thesis Co-Advisor
(Krissanapong Manotham, M.D.)
.....Examiner
(Assistant Professor Supang Maneesri le grand, Ph.D.)
.....Examiner
(Associate ProfessorPadet Siriyasatien, M.D., Ph.D.)
.....External Examiner
(Associate Professor Thawornchai Limjindaporn, M.D., Ph.D.)

CONTENTS

LIST OF FIGURES

Page

LIST OF TABLES

Page

CHAPTER I
BACKGROUND

Silver nanoparticles (AgNPs) are one of the most widely used nanoparticles in biomedical and industrial fields because of their antimicrobial properties. Various consumer products containing AgNPs have been developed over many decades, such as sterile medical devices, dermatological products, surface cleaners, and food storage containers.[1,2] However, the toxic effects of AgNPs have recently been raised concerns. It has been reported that AgNPs can enter the body through many routes of exposure, translocate into the bloodstream, and accumulate in particularly the liver and kidneys.[3] The kidney is one of the main excretory organs that removes metabolic wastes, absorbs minerals, and produces hormones. Therefore, aberrations of the kidney can lead to many serious conditions.

Even though AgNP toxicity is well characterized, methods to prevent the toxic effects remain unknown. Previous studies have revealed that AgNPs can induce cellular apoptosis through the mitochondrial dependent apoptosis pathway that involves down-regulation of the pro-survival protein Bcl-2.[4] Many reports showed that the main mechanisms of AgNP-induced damage in mammalian cells are mediated by increases in the level of intracellular reactive oxygen species (ROS).[5,6] Interestingly, this is the same mechanism through which AgNPs induce toxicity in microbes.[7] Using a general antioxidant to reduce ROS and prevent toxicity also reduces the ability of AgNPs to kill microbes. To optimize AgNPs for killing microbes without toxicity to mammalian cells, a cytoprotective compound is needed to exert antioxidative effects only in mammalian cells.

In this study, we aimed to develop a method to prevent the toxicity of AgNPs for broader and reliable use. Erythropoietin (EPO) and its derivatives have shown benefits in protection of various cells and tissues against acute and chronic injuries.[8-12] Recently, many researchers have focused on derivatives of EPO because they exert comparative cytoprotective effects with less adverse side effects such as overproduction of red blood cells.[13] Glutaraldehyde erythropoietin (GEPO), a modified form of EPO, is decidedly one of the most outstanding candidates in terms of protection against cellular injury. This compound was found to exert the same renoprotective effects as EPO both in vitro and in vivo. In addition, GEPO prevents kidney damage by increasing the expression of Bcl2 protein.[14]

The cytoprotective effects of GEPO led to our hypothesis that the cytotoxic activity of AgNPs toward renal cells would be ameliorated by applying this compound. Therefore, this study aimed to evaluate the cytoprotective effects of GEPO on a renal cell line (HEK293) with cytotoxicity induced by AgNPs.

CHAPTER II
LITERATURE REVIEW

Silver nanoparticles toxicity

Nanomaterials are objects or structures ranging from 1-100 nm in size and because of their specific physicochemical properties, they have been extensively applied in area of research and industry. One of the most common nanomaterials is silver nanoparticle (AgNP) which has been used as a major component in many consumer products.[4] There is an abundant amount of medical products and products in everyday life contain AgNPs by virtue of their bactericidal function and antimicrobial activity.[15] However, the toxicity of AgNPs in living organism is also remain an argumentative in the area of research.

The used of nanosilver in commercial products is increasing more interest; as a result, human exposure to AgNP become a part of our daily life. Due to its very small size, AgNP may be absorbed into the human body then penetrated through the blood stream and distributed to many tissues. The distribution of AgNPs in the blood circulation and the accumulation of AgNPs in tissues and organs can induce toxicity. Although the body has excretion process, the experimental in rats showed the residual of AgNPs in various organs extraordinarily in liver and kidney as show in figure 1.[3]

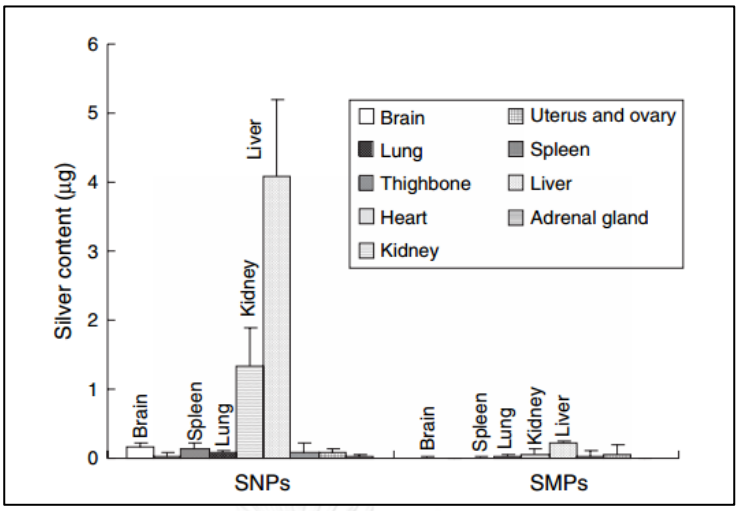

Figure 1: Silver particles distribution in different organs[3]

The mechanisms of AgNP uptake into the cell are pinocytosis, endocytosis dependent on caveolae and lipid raft composition, clathrin-dependent endocytosis and phagocytosis.[16] There are many factors affecting to the uptake kinetic of AgNP; for example, size and surface coat. In vitro experiment showed 20 nm AgNP are taken up into the cell mainly by endocytosis and appear inside the cell after 2 hr exposure. Since the excretion rate is less than internalization, some of AgNPs are remain inside the cell.[5] The intracellular localization of AgNP can be summated from the previous review as presented in figure 2.

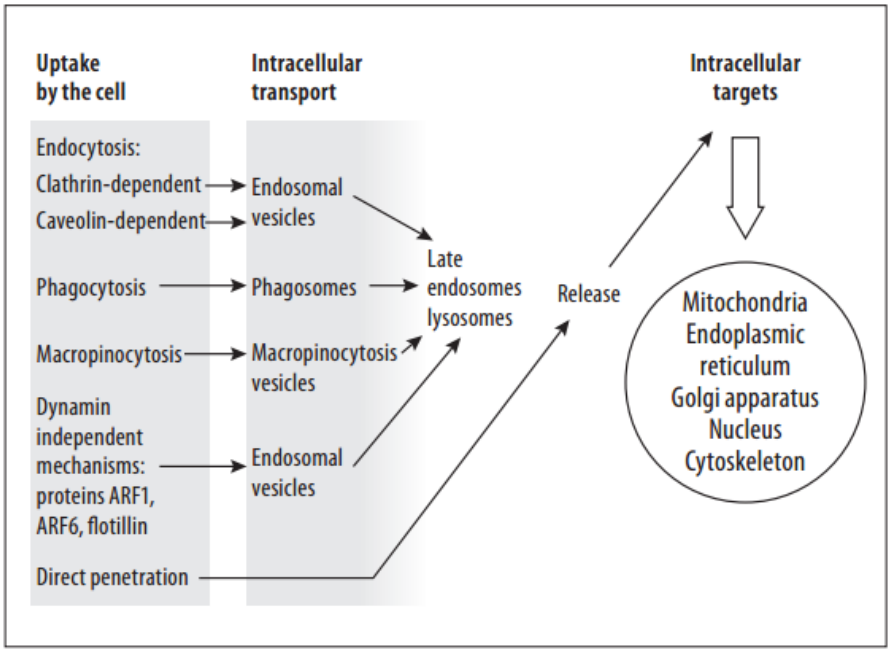

Figure 2: Diagram showing the AgNP uptake, transport pathways inside the cell and cellular targets.[5]

As mentioned above that the negative consequence after exposure to AgNPs can happen. According to this consideration, there are numerous of AgNPs toxicity study. The studies conducted the experiment on both *in vitro* and *in vivo* models as summarized from the previous review as showed in table 1 and 2.[17]

Table 1: In vitro models for AgNP toxicity assessment[17]

Size (nm)	Surface coating	Model	Concentration tested	Exposure duration	Outcome
10.88 (PVA) 5.78 (starch)	PVA coated, starch coated	Human erythrocytes	25–400 mg/ml	3 h	Produced more severe effects than uncoated
30–50	PVP-coated Ag (0.2% PVP)	A549 human lung carcinoma cells	0–20 mg/l	24 h	ROS generation and apoptosis
18	Uncoated	Baby hamster kidney (BHK21) and human colon adenocarcinoma (HT29) cells	11 mg/ml	12, 24 h	AgNPs induced p53-mediated apoptosis
730.5	Cellulose gumcoated	Human skin, HaCaT normal human keratinocytes	0.5, 50 ppm (skin), 0.002 – 0.02 ppm (cells)	24 h	AgNPs did not sensitize keratinocytes to UV-B radiation
13	Uncoated	Mouse blastocysts	25 and 50 mM	24 h	Embryonic toxicity
61	Uncoated	MAMCs primary culture murine adrenal medullary chromaffin cells	0.01, 0.1, and 1 nM	24 and 48 h	Cytotoxicity, decreased secretion
68.9	Uncoated	RAW264.7 mouse peritoneal macrophages	0.2–1.6 ppm	24, 48, 72, and 96 h	Cytotoxicity and oxidative stress
20, 50, 80 (uncoated)	Unwashed, washed, carbon coated	HEKs, human epidermal keratinocytes	0.000544–1.7 mg/ml	24 h	Dose-dependent decrease in cell viability of uncoated nanoparticles
30 (spherical)	Uncoated	Japanese medaka (Oryzias latipes) cell line	0.05–5 mg/cm^2	24 h	Toxicity, DNA damage
7–20	Uncoated	Mouse fibroblasts and liver cells	10–200 mg/ml	24 h	Reduced cell viability, oxidative stress, and apoptosis
35 (0.6–1.6 mm bulk)	Uncoated	C3A human hepatocytes, Caco-2 colon cancer cells Primary trout hepatocytes	0–1000 mg/ml	24 h	Internalization, cytotoxicity
100 (spherical)	PVP coated	hMSCs human mesenchymal stem cells	0.05–50 mg/ml	7 days	Cell proliferation and chemotaxis were decreased, while IL8 release was increased
50	Uncoated	Bovine retinal endothelial cells	100–500 nM	24 h	Induction of CASP3 activity and DNA ladder formation
5–10	Uncoated	HepG2 human hepatoma cells	0.1–5 mg/ml	28 h	Cytotoxicity, overexpression of superoxide dismutase, glutathione peroxidase, catalase

Table 2: In vivo mammalian models for AgNP toxicity assessment[17]

Size (nm)	Surface coating	Model	Concentration tested	Exposure method and duration	Outcome
18	None	Sprague–Dawley rats	1.73×10^4, 1.27×10^5, 1.32×10^6 particles/cm^3	Inhalation exposure: 6 h/day, 5 days/ week, for 28 days	No significant changes in the hematological and blood biochemical parameters in either male or female rats
18	None	Sprague–Dawley rats	1.73×10^4, 1.27×10^5, 1.32×10^6 particles/cm^3	Inhalation exposure: 6 h/day, 5 days/ week, for 90 days	Decreased tidal volume and alveolar inflammation. Increased bile duct hyperplasia and liver inflammation
18	None	Sprague–Dawley rats	30, 300, and 1000 mg/kg	Ingestion exposure: Ag NPs mixed with diet for 28 days	Significant dose-dependent changes in alkaline, phosphatase activity, cholesterol level, and slight liver damage
29	None	C57BL/6N mice	100, 500, and 1000 mg/kg	Intraparentally 24 h	Altered gene expression associated with oxidative stress in the caudate, frontal cortex, and hippocampus regions of the brain
13–15	None	Sprague–Dawley rats	1.73×10^4, 1.27×10^5, 1.32×10^6 particles/cm^3 (61 mg/m^3)	Inhalation exposure: 6 h/day, 5 times/ week, 28 days	Size and number of goblet cells containing neutral mucins increased in lungs
22	None	C57BL/6 mice	1.91×10^7 particles/cm^3	Inhalation exposure: 6 h/day, 5 days/ week, 14 days	Expression of several genes in the brain associated with motor neuron disorders, neurodegenerative disease, and immune cell function
56	None	Fischer F344 rats	30, 125, and 500 mg/kg body weight	Ingestion 90 days	Different adverse effects, including loss of body weight, changes in blood biochemical parameters, bile-duct hyperplasia, fibrosis, and pigmentation. Gender-related differences in accumulation of AgNPs in kidney
15	None	Fischer F344 rats	Inhalation 133 mg/m^3 (3×10^6 cm^3) Intratracheal 50 mg AgNPs 7 mg $AgNO_3$	Inhalation: 6 h Intratracheal: Single administration	Dose-dependent translocation to main organs
22, 42, 71, and 323	None	Mice	Single dose: 1 mg/kg Repeated doses: 0.25, 0.50, 1.00 mg/kg	Ingestion 14 days Repeated oral toxicity during 28 days (42 nm only)	Single dosage: The largest AgNPs were not found in any of the organs studied. Repeated dosage adversely impacts on liver and kidney in a high dosetreated group (1.00 mg/kg), when determined by blood chemistry and histopathological analysis. Decrease in cytokine levels

Attemps to clarify the mechanisms of AgNPs toxicity lead to the conclusion that AgNPs induce toxicity mainly through the induction of oxidative stress. One of the initial mechanisms of AgNPs to induce toxicity also involves with the alterations of mitochondria structure. The alteration of mitochondria mediated by AgNPs leads to induction of the production of reactive oxygen species (ROS).[4, 5, 17-19]As far as we know, ROS are involved in pathogenesis of various diseases and also play an important role in molecular pathways leading to the inducing cellular oxidative stress and increase level of proinflamatory cytokine production. The oxidative stress and inflammation as a consequence of AgNPs exposure have been found related to genotoxicity, cytotoxicity and cell death.[5, 17, 18]

Nanomaterial can cause cell death by activate through the different type of programmed cell death pathway. Mitochondria-dependent (intrinsic) apoptosis pathway appears to be main mechanism that AgNPs mediated cell death[1]. The characteristic of this pathway is the insertion of Bax and/or Bak proteins into the mitochondrial outer membrane in response to a wide range of apoptotic stimuli. The proteins from the mitochondrial intermembrane space such as cytochrome c, Apaf-1 and caspase 9 then forms a multi-protein complex know as apoptosome. Finally, the activation of an effector caspase leads to cell death. These processes are subsequently inhibited by antiapoptotic protein Bcl-2 as shown in figure 3.[4]

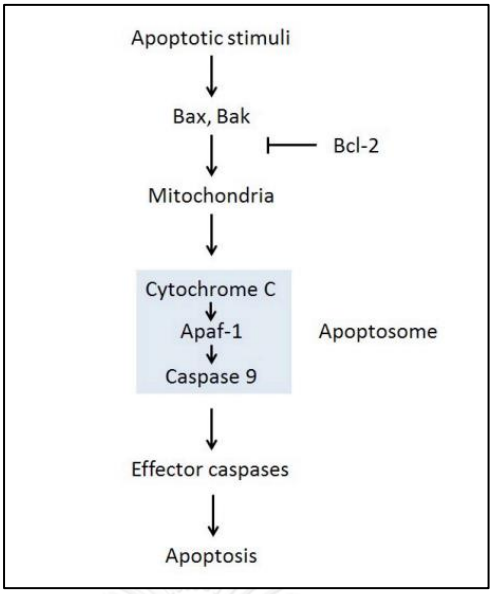

Figure 3: Schematic overview of main events in intrinsic apoptosis.[4]

Many recent studies using cell culture models to define mechanism of AgNPs toxicity. Factors responsible for nanosilver mediated apoptosis via intrinsic mitochondria-dependent pathway were investigated. The researchers found that AgNPs exposure induced the release of cytochrome c into the cytosol and translocation of Bax protein into mitochondrial. Nanosilver-induced apoptosis was associated with the generation of reactive oxygen species (ROS) and JNK activation, and inhibition of either ROS or JNK attenuated nanosilver-induced apoptosis.[20] In nanosilver-resistant HCT116 cells, up regulation of the anti-apoptotic proteins, Bcl-2 appeared to be associated with a diminished apoptotic response. Taken together, Zou's results provide the first evidence for a molecular mechanism of nanosilver cytotoxicity, showing that nanosilver acts through ROS and JNK to induce apoptosis via the mitochondrial pathway.[21]

Erythropoietin cytoprotection

Erythropoietin (EPO), a 165 amino acid glycoprotein hormone that produced 90% from kidney and about 10% from liver, regulates production and maturation of red blood cell. EPO in regard to medicine has been used to treat anemia in patient with chronic kidney disease.[22] It has been reported to protect various organs from acute and chronic injuries.[23-25]A concern was been raised about disadvantages of EPO treatment such as high levels of red blood cell in bloodstream, so a tissue-protective compounds which have cytoprotective effect without increasing red blood cell production is produced. Such compound is glutaraldehyde EPO (GEPO), the chemical targeted lysine modifications of erythropoietin.[14] Recently, many articles have been reported about modified form of recombinant human EPO that has the potential to reduce cellular oxidative stress and inflammation.[26, 27] These compound is a remarkable compound that has widespread usage in protecting various tissues. This has been shown by multiple workers through different model systems in both in vitro and in vivo. [28]

EPO was classified as a type I cytokine that require recognition by its receptor and decode into specific intracellular signaling cascades to exert its biological effects. The tissue protective compound including modified form of recombinant human EPO has been reported to exerts protective effect via three dominant signaling pathways through the beta common receptor / erythropoietin receptor. The initial step after this tissue protective molecule binds to the receptor is autophosphorylation of JNK2 molecule. Following the JAK2 phosphorylation, (1) the STAT pathway are activated. The activation of STAT pathway leads to increased in survival signals. (2) A second pathway is PI3K/Akt pathway, which the critical protective pathway in liver and

kidney. (3) A third pathway is mitogen-activated protein kinases or MAPKs pathway as shown in figure 4. Activation of both PI3K/Akt and MAPKs pathways by the tissue protective molecule have been found to directly stabilize mitochondria and subsequent inhibition of death signals.[29] In addition, the anti-apoptotic effect of nonhematopoietic erythropoietin derivative, GEPO, administration has been shown the potential renoprotective properties both in vitro and in vivo conditions.[14]

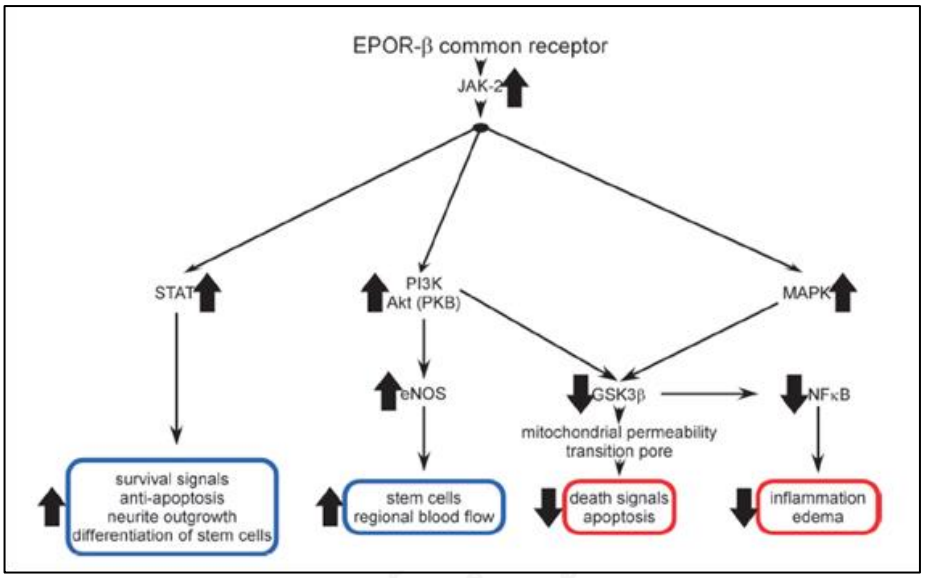

Figure 4: Multiple signaling pathways have been documented for the tissue protective Receptor[29].

Therefore, the aim of this study is to focus on the cytoprotective effect of GEPO in AgNPs-induced kidney cell injury. In this regard, the mechanisms underlying of GEPO in protect cellular apoptosis was evaluated.

CHAPTER III
MATERIALS AND MEDTHODS

Characterization of AgNPs

Commercial nanosilver in aqueous buffer, which contained sodium citrate as a stabilizer, was purchased from Sigma-Aldrich (St. Louis, MO, USA). The absorption wavelength of AgNPs was primarily determined using a UV spectrophotometer (Beckman Coulter, Miami, FL, USA). To characterize the particle size and shape, a AgNP solution was analyzed in a carbon-coated copper grid by a Hitachi H-7650 transmission electron microscope equipped with a CCD camera (Hitachi High-Technologies Corporation, Tokyo, Japan).

Cell culture

Human embryonic kidney cells (HEK293) were cultured in Dulbecco's modified Eagle's medium (DMEM) supplemented with 10% fetal bovine serum and 1% penicillin-streptomycin. The cells were grown in 75-cm^2 culture flasks at 37°C in a 5% CO_2 incubator.

Cytotoxicity assay

Because living cells express mitochondrial dehydrogenase, detecting the level of this enzyme was used to assess cell survival. Cell viability assays were conducted in 96-well plates. A total of 5×10^3 cells in 45 µL DMEM were seeded into each well and incubated overnight at 37°C with 5% CO_2. To determine the dose for induction of cytotoxicity by AgNPs , HEK293 cells were treated with AgNPs at various

concentrations (1–100 μg/mL) for 4 hours. The treatment concentration of AgNPs was determined by the half maximal inhibitory concentration (IC_{50}) value. Then, assessment of cytoprotection by GEPO were performed by the following treatments: (1) negative control (DMEM only), (2) AgNPs, (3) GEPO-pretreatment before addition of AgNPs, and (4) EPO pretreatment prior to administration of AgNPs. Six replicates were included for each sample. PrestoBlue™ reagent (Invitrogen, Carlsbad, CA, USA), a cell-permeable compound that becomes highly fluorescent through reduction by dehydrogenase, was then added to each well, followed by incubation for 30 minutes. Cell viability was determined by measurement of the fluorescence intensity using a microplate reader at 530 nm excitation and 590 nm emission.

Morphological evaluation

To analyze changes in cell morphology, HEK293 cells were seeded in 24-well plates at a density of 5×10^4 cells/well and incubated at 37°C with 5% CO_2 for 24 hours. Cells cultured in medium alone were used as a negative control. Alterations in cell morphology were assessed in cells treated with 20 μg/mL AgNPs and compared with cells pretreated with 0.42 μg/mL GEPO before addition of AgNPs using a phase contrast microscope (Eclipse TS 100, Nikon, Tokyo Japan) and transmission electron microscope (Hitachi).

Death pattern analysis

The pattern of cell death was determined by flow cytometry (FACSCalibur; Becton-Dickinson, San Jose, CA, USA) after staining with FITC-conjugated annexin V and propidium iodide (PI) (BD Biosciences, San Jose, CA, USA) according to the

manufacturer's instructions. Briefly, cells were collected by trypsinization, washed twice with cold phosphate-buffer saline (PBS), and resuspended in annexin V binding buffer. FITC-conjugated annexin V and PI working solutions were added to the tube containing the collected cells, followed by incubation in the dark at room temperature (25°C) for 15 minutes. Stained HEK293 cells were analyzed within 1 hour after staining by the FACSCalibur using emission filters for FITC at 530/30 nm and PI at 585/42 nm. The percentage of cells undergoing different types of cell death were analyzed by CellQuest software (Becton Dickinson).

Real-time PCR analysis

For the cell proliferation assay, Ki-67 gene expression was used to indicate cell cycle progression. Total RNA were isolated from the cells with TRIzol® Reagent (Life Technologies, Carlsbad, CA, USA) and quantified by a micro-volume spectrophotometer at 260 nm. cDNA was synthesized in a 20 µl reaction using a RevertAid™ First Strand cDNA Synthesis Kit (Thermo Scientific, Waltham, MA, USA) according to the manufacturer's instructions. To analyze gene expression in the real-time PCR system (StepOnePlus, ABI Applied Biosystems), and used Express SYBR® GreenER™ qPCR Supermix Kit (Invitrogen, Carlsbad, CA, USA). The threshold cycle values for Ki-67 gene amplification were normalized to the endogenous housekeeping gene (GAPDH) expression level in relation to the calibrator.

ROS generation

To evaluate intracellular ROS levels, we used 2',7'-dichlorodihydrofluorescein diacetate (DCFH-DA) reagent (Invitrogen, USA). The cells were treated under the same conditions as those for the cell viability assay. HEK293 cells growing in black 96-well plates were treated with DCFH-DA reagent for 30 minutes in the dark. After nonfluorescent DCFH-DA reagent penetrates into cells, esterases within the cells initiate hydrolysis of DCFH-DA to 2',7'-dichlorodihydrofluorescein (DCFH). 2',7'-Dichlorofluorescein (DCF) produced by oxidation of DCFH in the presence of ROS was immediately detected using a fluorescence microplate reader at a excitation wavelength of 485 nm and emission wavelength of 528 nm. The emission intensity of the AgNP-treated group was measured and compared with the GEPO-pretreated group.

Western blotting

The expression of Bcl2 protein was examined by western blot analysis. Cell lysates were centrifuged and the supernatants were collected. The total protein concentration was determined using a BCA protein assay kit (Thermo Scientific, Rockford, IL, USA). For immunoblotting, the proteins were loaded onto a polyacrylamide gel and separated by electrophoresis. Then, the separated proteins were transferred to a PVDF membrane. The membrane was incubated with a primary anti-Bcl2 antibody (Santa Cruz Biotechnology, Santa Cruz, CA, USA) at an optimal overnight at 4°C. After three washes, the membrane was incubated with a goat anti-rabbit secondary antibody (Santa Cruz Biotechnology, Santa Cruz, CA, USA) conjugated with horseradish peroxidase for 1 hour. The immunoreactive bands were

visualized using an enhanced chemiluminescence western blot substrate. Equal loading of proteins was confirmed by measuring β-actin

CHAPTER IV
RESULTS AND DISCUSSION

RESULTS

Characterization of Silver nanoparticles

Commercial AgNPs were characterized by transmission electron microscopy (TEM) and a UV-Vis spectrometer. The particles had a spherical shape and mean size of 10 nm (Figure 5A). The maximum absorption wavelength was 403 nm that corresponded to the yellow color of the AgNP dispersion (Figure 5B).

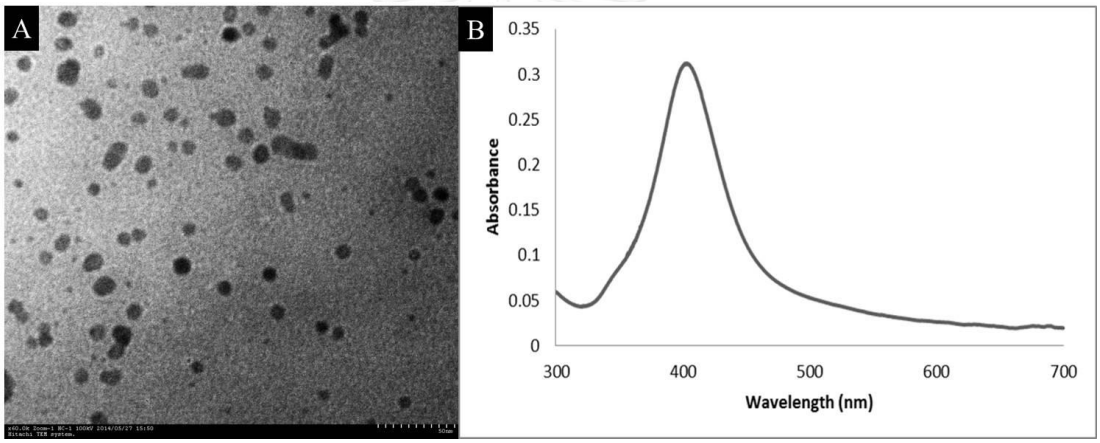

Figure 5: Characterization of AgNPs by TEM (A) and spectroscopy (B).

Cytotoxic effects of AgNPs on HEK293 cells

The dose-dependent cytotoxic effect of AgNPs on HEK293 cells was examined by a PrestoBlue™ cell viability assay. HEK293 cells were exposed to AgNPs at concentrations of 1–100 μg/mL for 4 hours. The IC_{50} was 19.74 μg/mL (Figure 6). In further experiments, the concentration of 20 μg/mL AgNPs was selected to assess protective effects of GEPO against AgNP-induced cell injury.

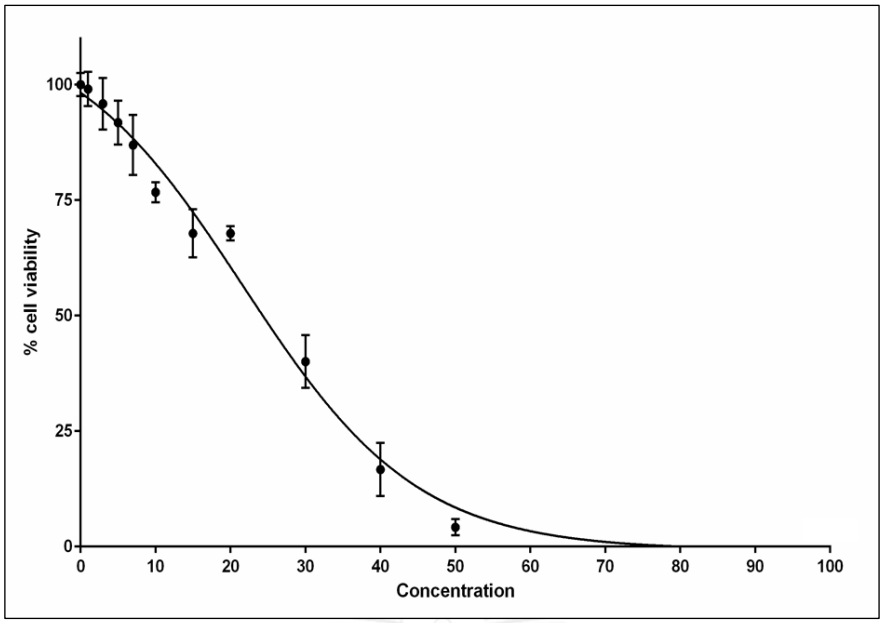

Figure 6: Effect of AgNPs on the viability of HEK293 cells at 4 hours of exposure.

Cell viability assay

We hypothesized that GEPO can inhibit the cytotoxicity of AgNPs. Thus, we pretreated HEK293 cells with GEPO and investigated the cell viability after exposure to AgNPs. As a result, the pretreated groups showed significantly higher cell viability than the non-pretreated group (Figure 7).

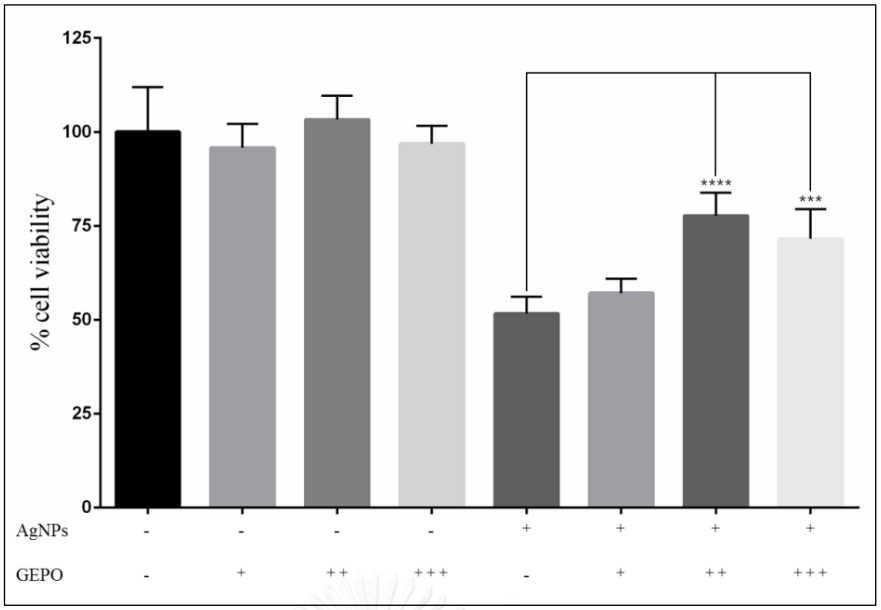

Figure 7: Percentage of viable cells following AgNPs exposure with or without GEPO pretreatment.

Cell morphology study

To determine whether AgNP-induced cytotoxicity was associated with an altered morphology of HEK293 cells, we evaluated the morphological changes of AgNP-exposed cells with and without GEPO pretreatment by phase contrast microscopy and TEM. Compared with the untreated group, AgNP-treated cells showed a distinct morphology and ultrastructural alterations. HEK293 cells after incubation with AgNPs under a light microscope showed cell shape became round, the number of cells decreased, and detached from the surface of the well plate (Figure 8). In addition, TEM analysis of AgNP-exposed cells revealed karyolysis and pyknosis characteristics including nuclear fading due to chromatin dissolution and shrinkage of the nucleus, respectively. These specific changes in nuclear morphology suggest the initial stage of apoptosis caused by cell damage. On the other hand,

GEPO-pretreated cells retained their normal cellular morphological characteristics as shown in both light microscopy and TEM analyses (Figure 9).

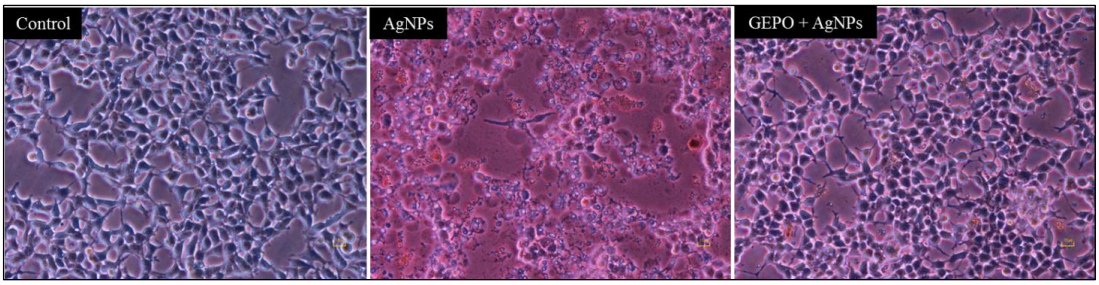

Figure 8: Effect of AgNPs and GEPO on cell morphology under light microscope.

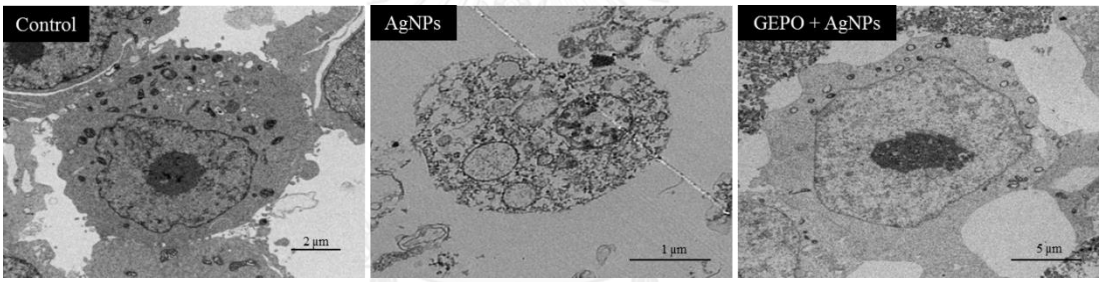

Figure 9: Effect of AgNPs and GEPO on cell morphology under transmission electron microscope.

Assessment of the cell death pattern

To confirm the involvement of GEPO in prevention of cell death, both FITC-conjugated annexin V and PI were employed to examine the pattern of cell death. The data showed the percentages of cells that were stained by either annexin V or PI or double-stained by both molecules to indicate cell death or the unstained cells that represent live cells. Cells treated with AgNPs had a higher the percentage of stained cells both the percentages of early apoptotic cells (63.58%) and late apoptotic cells (21.22%) than GEPO pre-treated cells (Figure 10).

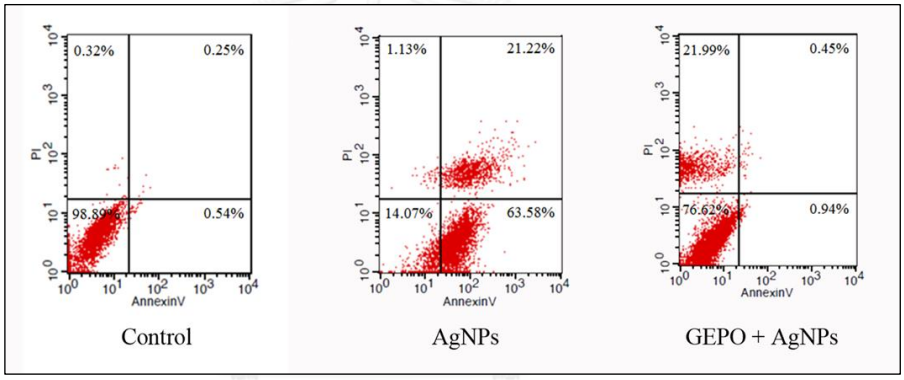

Figure 10: Death pattern analysis of cells treated with DMEM only, AgNPs, or pretreated with GEPO before administration of AgNPs.

GEPO restores the proliferative ability of cells

To confirm that GEPO maintains the normal proliferation of cells, the expression of Ki-67, which is a marker of cells undergoing proliferation, was evaluated by real-time RT-PCR (Figure 11). The level of Ki-67 expression in AgNP-exposed cells was unchanged, whereas that in GEPO-pretreated cells before exposure to AgNPs was increased significantly.

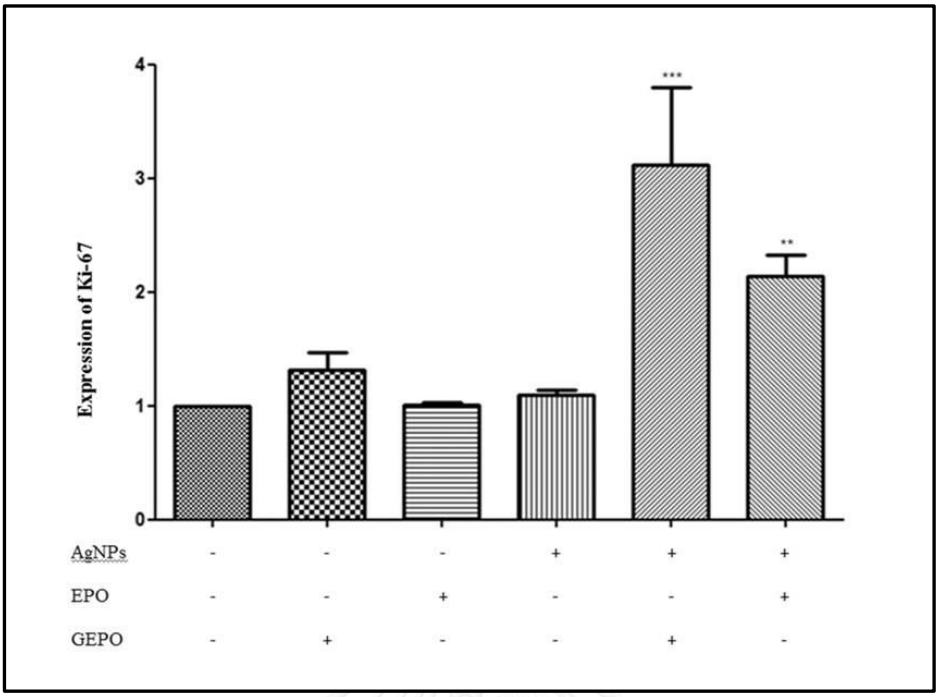

Figure 11: Detection of KI-67 mRNA expression in HEK293 cells exposed to AgNPs with and without GEPO or EPO pretreatment.

Effect of silver nanoparticle on ROS generation

The ROS generation of HEK293 cells in the presence of AgNPs was evaluated using DCFH-DA technique. After HEK 293 cells were incubated with various concentrations of AgNPs, the level of ROS was detected using a fluorescence microplate reader. The result showed that AgNPs are able to increase the ROS generation in HEK293 cells in a dose dependent manner (Figure 12).

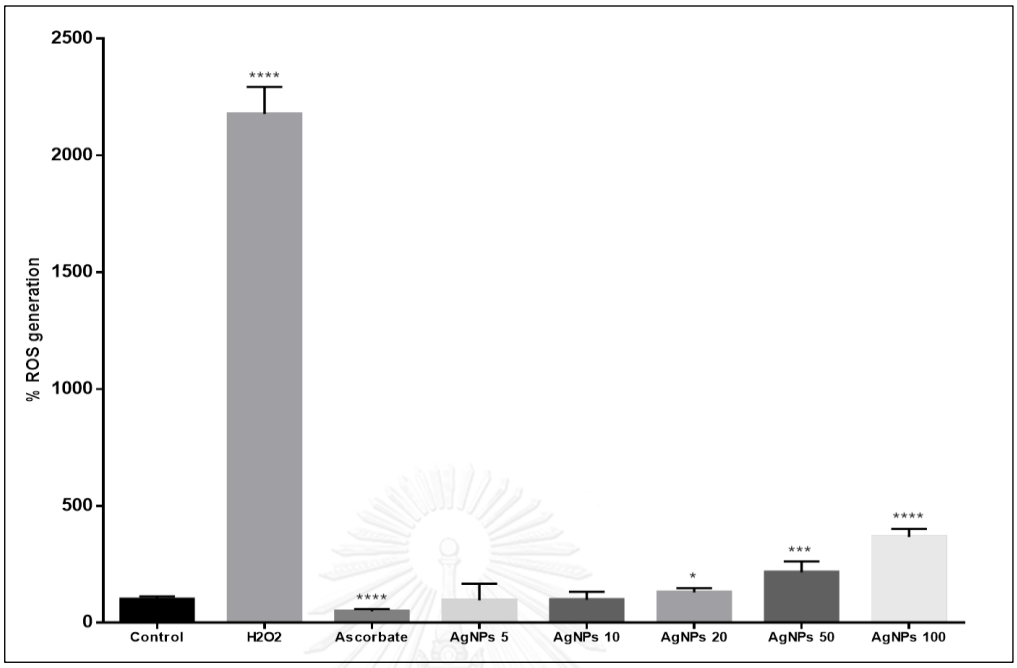

Figure 12: Evaluation of ROS generation in HEK293 cells exposed to AgNPs in a dose dependent manner.

GEPO exerts cytoprotective effects via amelioration of ROS

AgNPs exert toxic effects on cells mainly by increasing ROS generation. To explore the role of GEPO in prevention of ROS production, we next investigated the level of ROS generation. HEK293 cells after treatment with AgNPs showed significant augmentation in the generation of ROS compared with the control group. However, the intracellular ROS, which generated by AgNP treatment, were substantially attenuated by GEPO pretreatment (Figure 13).

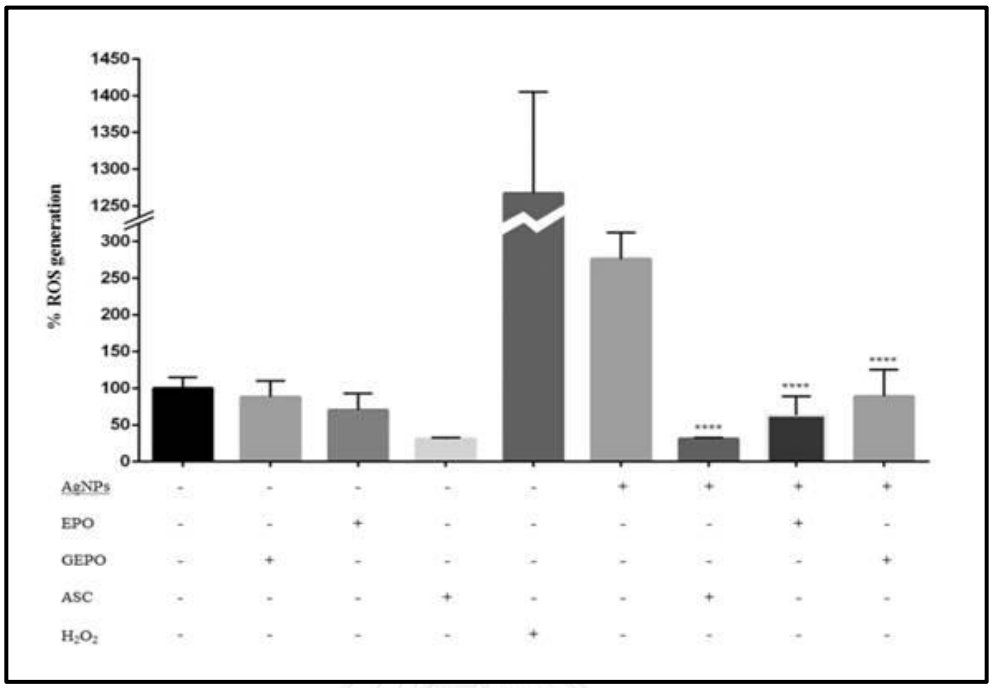

Figure 13: ROS generation of HEK293 cells in the presence of AgNPs with and without GEPO or EPO pretreatment.

GEPO exerts cytoprotective effects by up-regulation of Bcl2

In our previous study, we revealed that administration of GEPO induces Bcl2 expression.[14] Accordingly, to evaluate the effect of GEPO on AgNP-exposed cells, western blot analysis was applied to measure Bcl2-protein expression. We found that AgNPs considerably inhibited the expression of Bcl2-protein, whereas cells pretreated with GEPO showed up-regulation of Bcl2-protein expression (Figure 14).

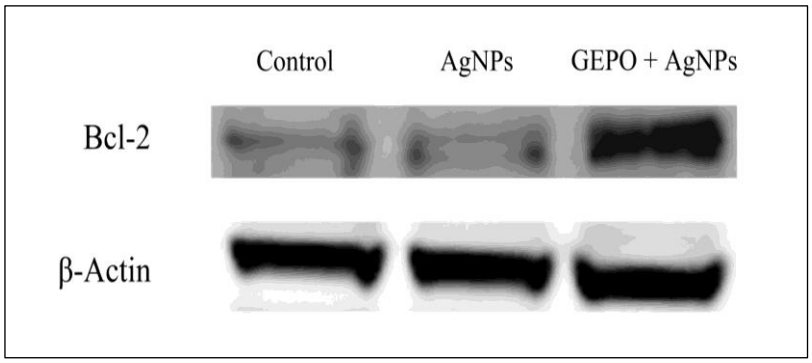

Figure 14: Western blot analysis of Bcl2 protein in AgNP-treated cells with or without GEPO pretreatment.

DISCUSSION

In this study, we investigated the effect of GEPO, a cytoprotective compound that has been shown to protect against renal cell apoptosis by up-regulation of Bcl2 protein as well as ameliorate kidney damage induced by ischemic/reperfusion conditions.[14] Our results revealed that AgNP-exposed cells had morphological damage, decreased cell viability, increased ROS generation, and down-regulated Bcl2 expression. Pretreatment with GEPO not only attenuated the ROS production, but also up-regulated Bcl2 expression, which probably contributed to rescuing the cellular damage induced by AgNPs. Therefore, GEPO possibly has a beneficial effect on AgNP-induced renal cell injury.

AgNPs are one of the most popular nanomaterials in many consumer products. The expansion in the use of nanosilver has led to an increase in the awareness of its toxicity.[30,31] AgNPs damage cells, which contributes to the generation of free radicals

and the consequential cellular oxidative stress and reduction in Bcl-2 protein expression.[30] Bcl-2 protein has a role in the antioxidant pathway and has been reported to protect cells against apoptosis induced by ROS.[32,33] Thus, an approach that possibly targets both the cellular stresses resulting from ROS generation and regulation of Bcl-2 protein expression is an appropriate strategy for the prevention and treatment of cellular injury caused by AgNPs.

Although it is unclear how GEPO prevents AgNP-induced cellular injury, our previous study showed that GEPO has a binding affinity for a tissue-protective receptor, the IL3RB/EPOR heterotrimeric receptor.[14] Under normal conditions, this tissue-protective receptor is not expressed, but appears when cells are exposed to noxious stimuli.[42] Tissue-protective compounds including modified forms of recombinant human EPO have been reported to exert protective effects via this receptor. [13,42,46] The initial step after these types of tissue-protective molecules bind to the IL3RB/EPOR heterotrimeric receptor is autophosphorylation of the JAK2 molecule. Following JAK2 phosphorylation, STAT, PI3K/Akt, and mitogen-activated protein kinase (MAPK) pathways are activated. The activation of these three pathways plays an important role in the regulation of mitochondrial integrity, activation of anti-apoptotic signals, and inhibition of pro-apoptotic molecules.[42] Therefore, it is possible that the cytoprotective effects of GEPO are mediated by activation of the IL3RB/EPOR heterotrimeric receptor.

The prominent features of cells after exposure to AgNPs are cytotoxicity including a reduction in cell viability, abnormal morphology, and an impairment in the ability to proliferate.[32, 47, 48] Previous reports have suggested that exposure to AgNPs causes cell cycle arrest.[37, 38] Conversely, based on our results, AgNPs had no

significant effect on cell proliferation compared with the control. Ahamed et al. found that the toxic effects of AgNPs are not only dependent on cell type-specific responses to this nanomaterial but are also related to concentration-dependent effects.[39] A low dose of AgNPs has anti-proliferative effects, whereas a high dose has been shown to activate cell proliferation.[40] These findings suggest that a toxic concentration of AgNPs may function as a molecular activator of proliferative pathways.

In our study, treatment of the renal cell line with GEPO promoted the cells to enter the active phase of the cell cycle. Interestingly, the level of proliferation observed in cells pretreated with GEPO and then treated with AgNPs was higher than that in cells treated with GEPO alone. It is likely that either both GEPO and AgNPs have the potential to increase cell proliferation independently or AgNPs might play a role in amplifying the proliferative effect of GEPO in the deleterious environments induced by AgNPs. A possible explanation for the combined effect of AgNPs and GEPO in the augmentation of renal cell proliferation is cross-regulation of the c-Jun N-terminal kinase (JNK) pathway by these two molecules. JNK is a member of the MAPK family and functions as a key molecular mediator in the activation of cell proliferation.[41,42] Activation of the JNK pathway has been reported to be triggered by cellular oxidative stress resulting from AgNPs and functions as a regulator in the activation of compensatory cell proliferation.[20, 43-45] Moreover, EPO has been found to potentially stimulate this pathway and consequently induce cell proliferation.[46,47]

We found an increase in the number of apoptotic cells among cells treated with AgNPs alone, whereas pretreatment with GEPO decreased the percentage of apoptotic cells. However, the pattern of cell death among cells pretreated with GEPO appeared to switch from apoptosis to necrosis. Previous studies have reported

that EPO and its derivative exert protective effects by inhibiting caspase-9 and 3 activities.[46,48] In addition, it has been revealed that the mechanism underlying the switch in the pattern of cell death is related to inhibition of caspases.[49,50] Based on these findings, we propose that GEPO reduces cell death not only by increasing expression of the anti-apoptotic protein Bcl2 but also by inhibition of caspases involved in apoptosis.

Based on our results, GEPO was found to exerted anti-oxidative effects. Pretreatment with GEPO before AgNP treatment diminished the induced ROS generation, one of the major causes of AgNP-induced cellular injury.[5,32] This is the first report to show that GEPO prevents ROS generation. We propose the possibility that GEPO acts in a similar manner as EPO. Previous studies have reported direct antioxidative effects of EPO in renal endothelial cells.[51,52] In addition, EPO increases antioxidative enzyme expression as well as up-regulates Nrf2 and heme oxygenase-1. [51-54] Up-regulation of Nrf2 and heme oxygenase-1 has significant protective effects against AgNP-induced cellular toxicity.[55,56]

The present study demonstrated the ability to prevent AgNP-induced cell injury by GEPO, which decreased ROS generation and stimulated Bcl2 expression. These findings increase our understanding of GEPO as a cellular protective compound and suggests a molecular mechanism of this agent. However, the mechanisms of action of GEPO in the reduction of ROS and activation of Bcl2 protein expression are still unknown. Further studies are needed to reveal the precise mechanism and the associated pathways of GEPO in protection against cellular toxicity induced by AgNPs.

CHAPTER V
CONCLUSION

In summary, our data confirmed that, under conditions of cellular oxidative stress and the consequential cytotoxicity induced by AgNPs, GEPO exhibited a cytoprotective function in the renal cell model. GEPO is able to reduce ROS generation and promote expression of the pro-survival protein Bcl2, which promoted cell survival. This finding sheds light on prevention of nanomaterial toxicity. The next step is to better understand the cell signaling processes that are specifically responsible for cell protection conferred by GEPO. Based on this knowledge, AgNPs can be potentially used without cellular toxicity, as least in human kidney cells.

REFERENCES

1. Ge L, Li Q, Wang M, Ouyang J, Li X, Xing MM. Nanosilver particles in medical applications: synthesis, performance, and toxicity. Int J Nanomedicine. 2014;9:2399–2407.
2. Wijnhoven SW, Peijnenburg WJ, Herberts CA, et al. Nano-silver-a review of available data and knowledge gaps in human and environmental risk assessment. Nanotoxicology. 2009;3(2):109–138.
3. Tang J, Xiong L, Wang S, et al. Distribution, translocation and accumulation of silver nanoparticles in rats. J Nanosci Nanotechnol. 2009;9(8):4924–4932.
4. Foldbjerg R, Autrup H. Mechanisms of silver nanoparticle toxicity. Arch Basic Appl Med. 2013;1(1):5–15.
5. Bartłomiejczyk T, Lankoff A, Kruszewski M, Szumiel I. Silver nanoparticles–allies or adversaries. Ann Agric Environ Med. 2013;20(1):48–54.
6. Patlolla AK, Hackett D, Tchounwou PB. Genotoxicity study of silver nanoparticles in bone marrow cells of Sprague-Dawley rats. Food Chem Toxicol. 2015 May 30. pii: S0278-6915(15)00170-2. doi: 10.1016/j.fct.2015.05.005
7. Pelgrift RY, Friedman AJ. Nanotechnology as a therapeutic tool to combat microbial resistance. Adv Drug Deliv Rev. 2013;65(13–14):1803–1815.
8. Liu X, Zhu B, Zou H, et al. Carbamylated erythropoietin mediates retinal neuroprotection in streptozotocin-induced early-stage diabetic rats. Graefes Arch Clin Exp Ophthalmol. 2015 Aug;253(8):1263–1272. Epub 2015 Mar 1.

9. Mofidi A, Bader A, Pavlica S. The use of erythropoietin and its derivatives to treat spinal cord injury. Mini Rev Med Chem. 2011;11(9):763–770.

10. Nguyen AQ, Cherry BH, Scott GF, Ryou MG, Mallet RT. Erythropoietin: powerful protection of ischemic and post-ischemic brain. Exp Biol Med (Maywood). 2014;239(11):1461–1475.

11. Wang Y, Lu X, He J, Zhao W. Influence of erythropoietin on microvesicles derived from mesenchymal stem cells protecting renal function of chronic kidney disease. Stem Cell Res Ther. 2015;6(1):100–100.

12. Sanchis-Gomar F, Garcia-Gimenez JL, Pareja-Galeano H, Romagnoli M, Perez-Quilis C, Lippi G. Erythropoietin and the heart: physiological effects and the therapeutic perspective. Int J Cardiol. 2014;171(2):116–125.

13. Van Rijt WG, Van Goor H, Ploeg RJ, Leuvenink HG. Erythropoietin-mediated protection in kidney transplantation: nonerythropoietic EPO derivatives improve function without increasing risk of cardiovascular events. Transpl Int. 2014;27(3):241–248.

14. Chattong S, Tanamai J, Kiatsomchai P, et al. Glutaraldehyde erythropoietin protects kidney in ischaemia/reperfusion injury without increasing red blood cell production. Br J Pharmacol. 2013;168(1):189–199.

15. Chen X, Schluesener H. Nanosilver: a nanoproduct in medical application. Toxicol Lett. 2008;176(1):1-12.

16. Zhao F, Zhao Y, Liu Y, Chang X, Chen C, Zhao Y. Cellular uptake, intracellular trafficking, and cytotoxicity of nanomaterials. Small. 2011;7(10):1322-37.

17. Kruszewski M, Brzoska K, Brunborg G, et al. Toxicity of silver nanomaterials in higher eukaryotes. Adv Mol Toxicol. 2011;5:179–218.

18. Johnston HJ, Hutchison G, Christensen FM, Peters S, Hankin S, Stone V. A review of the in vivo and in vitro toxicity of silver and gold particulates: particle attributes and biological mechanisms responsible for the observed toxicity. Crit Rev Toxicol. 2010;40(4):328-46.

19. McShan D, Ray PC, Yu H. Molecular toxicity mechanism of nanosilver. J Food Drug Anal. 2014;22(1):116-27

20. Hsin YH, Chen CF, Huang S, Shih TS, Lai PS, Chueh PJ. The apoptotic effect of nanosilver is mediated by a ROS- and JNK-dependent mechanism involving the mitochondrial pathway in NIH3T3 cells. Toxicol Lett. 2008;179(3):130-9.

21. Zou J, Feng H, Mannerström M, Heinonen T, Pyykkö I. Toxicity of silver nanoparticle in rat ear and BALB/c 3T3 cell line. J Nanobiotechnology. 2014;12(1):52.

22. Drueke TB. Anemia treatment in patients with chronic kidney disease. N Engl J Med. 2013;368(4):387-9.

23. Letourneur A, Petit E, Roussel S, Touzani O, Bernaudin M. Brain ischemic injury in rodents: the protective effect of EPO. Methods Mol Biol (Clifton, NJ). 2013;982:79-101.

24. Luo W, Hu L, Wang F. The Protective Effect of Erythropoietin on the Retina. Ophthalmic Res. 2015;53(2):74-81.

25. Shen S, Jin Y, Li W, Liu X, Zhang T, Xia W, et al. Recombinant human erythropoietin pretreatment attenuates acute renal tubular injury against ischemia-reperfusion by restoring transient receptor potential channel-6 expression and function in collecting ducts. Crit Care Med. 2014;42(10):e663-72.

26. Simon F, Scheuerle A, Groger M, Vcelar B, McCook O, Moller P, et al. Comparison of carbamylated erythropoietin-FC fusion protein and recombinant human erythropoietin during porcine aortic balloon occlusion-induced spinal cord ischemia/reperfusion injury. Intensive Care Med. 2011;37(9):1525-33.

27. Nijboer WN, Ottens PJ, van Dijk A, van Goor H, Ploeg RJ, Leuvenink HG. Donor pretreatment with carbamylated erythropoietin in a brain death model reduces inflammation more effectively than erythropoietin while preserving renal function. Crit Care Med. 2010;38(4):1155-61.

28. Brines M, Cerami A. Erythropoietin-mediated tissue protection: reducing collateral damage from the primary injury response. J Intern Med. 2008;264(5):405-32.

29. Brines M, Cerami A. The receptor that tames the innate immune response. Mol Med. 2012;18(1):486-96.

30. Dubey P, Matai I, Kumar SU, Sachdev A, Bhushan B, Gopinath P. Perturbation of cellular mechanistic system by silver nanoparticle toxicity:

Cytotoxic, genotoxic and epigenetic potentials. Adv Colloid Interface Sci. 2015;221:4–21.

31. Gaillet S, Rouanet JM. Silver nanoparticles: their potential toxic effects after oral exposure and underlying mechanisms—a review. Food Chem Toxicol. 2015;77:58–63.

32. Hockenbery DM, Oltvai ZN, Yin XM, Milliman CL, Korsmeyer SJ. Bcl-2 functions in an antioxidant pathway to prevent apoptosis. Cell. 1993;75(2):241–251.

33. Hildeman DA, Mitchell T, Aronow B, Wojciechowski S, Kappler J, Marrack P. Control of Bcl-2 expression by reactive oxygen species. Proc Natl Acad Sci U S A. 2003;100(25):15035–15040.

34. Yang C, Zhao T, Lin M, et al. Helix B surface peptide administered after insult of ischemia reperfusion improved renal function, structure and apoptosis through beta common receptor/erythropoietin receptor and PI3K/Akt pathway in a murine model. Exp Biol Med (Maywood). 2013;238(1):111–119.

35. Brzoska K, Meczynska-Wielgosz S, Stepkowski TM, Kruszewski M. Adaptation of HepG2 cells to silver nanoparticles-induced stress is based on the pro-proliferative and anti-apoptotic changes in gene expression. Mutagenesis. 2015;30(3):431–439.

36. Bhakat C, Chetal G, Sarkar P, Singh P, Babu S, Reddy A. Effects of silver nanoparticles synthesize from ficus benjamina on normal cells and cancer cells. IOSR J. Pharm. Biol. Sci. 2012;1:33–36.

37. Kang SJ, Lee YJ, Lee EK, Kwak MK. Silver nanoparticles-mediated G2/M cycle arrest of renal epithelial cells is associated with NRF2-GSH signaling. Toxicol Lett. 2012;211(3):334–341.

38. Lee YS, Kim DW, Lee YH, et al. Silver nanoparticles induce apoptosis and G2/M arrest via PKCzeta-dependent signaling in A549 lung cells. Arch Toxicol. 2011;85(12):1529–1540.

39. Ahamed M, Alsalhi MS, Siddiqui MK. Silver nanoparticle applications and human health. Clin Chim Acta. 2010;411(23-24):1841–1848.

40. Rosas-Hernandez H, Jimenez-Badillo S, Martinez-Cuevas PP, et al. Effects of 45-nm silver nanoparticles on coronary endothelial cells and isolated rat aortic rings. Toxicol Lett. 2009;191(2-3):305–313.

41. Hui L, Bakiri L, Mairhorfer A, et al. p38alpha suppresses normal and cancer cell proliferation by antagonizing the JNK-c-Jun pathway. Nature. 2007;39(6):741–749.

42. Sabapathy K, Hochedlinger K, Nam SY, Bauer A, Karin M, Wagner EF. Distinct roles for JNK1 and JNK2 in regulating JNK activity and c-Jun-dependent cell proliferation. Mol Cell. 2004;15(5):713–725.

43. Satapathy SR, Mohapatra P, Das D, Siddharth S, Kundu CN. The apoptotic effect of plant based nanosilver in colon cancer cells is a p53 dependent process involving ROS and JNK cascade. Pathol Oncol Res. 2015;21(2):405–411.

44. Fan Y, Bergmann A. Apoptosis-induced compensatory proliferation. The Cell is dead. Long live the Cell!. Trends Cell Biol. 2008;18(10):467–473.

45. Ryoo HD, Gorenc T, Steller H. Apoptotic cells can induce compensatory cell proliferation through the JNK and the wingless signaling pathways. Dev Cell. 2004;7(4):491–501.

46. Jacobs-Helber SM, Ryan JJ, Sawyer ST. JNK and p38 are activated by erythropoietin (EPO) but are not induced in apoptosis following EPO withdrawal in EPO-dependent HCD57 cells. Blood. 2000;96(3):933–940.

47. Jacobs-Helber SM, Sawyer ST. Jun N-terminal kinase promotes proliferation of immature erythroid cells and erythropoietin-dependent cell lines. Blood. 2004;104(3):696–703.

48. Chong ZZ, Kang JQ, Maiese K. Apaf-1, Bcl-xL, cytochrome c, and caspase-9 form the critical elements for cerebral vascular protection by erythropoietin. J Cereb Blood Flow Metab. 2003;23(3):320–330.

49. Nikoletopoulou V, Markaki M, Palikaras K, Tavernarakis N. Crosstalk between apoptosis, necrosis and autophagy. Biochim Biophys Acta. 2013;1833(12):3448–3459.

50. Lemaire C, Andréau K, Souvannavong V, Adam A. Inhibition of caspase activity induces a switch from apoptosis to necrosis. FEBS Lett. 1998;425(2):266–270.

51. Katavetin P, Tungsanga K, Eiam-Ong S, Nangaku M. Antioxidative effects of erythropoietin. Kidney Int. 2007;72:S10–S15.

52. Katavetin P, Inagi R, Miyata T, et al. Erythropoietin induces heme oxygenase-1 expression and attenuates oxidative stress. Biochem Biophys Res Commun. 2007;359(4):928–934.

53. Jin W, Kong J, Lu T, et al. Erythropoietin prevents secondary brain injury induced by cortical lesion in mice: possible involvement of Nrf2 signaling pathway. Ann Clin Lab Sci. 2011;41(1):25–32.

54. Genc K, Egrilmez MY, Genc S. Erythropoietin induces nuclear translocation of Nrf2 and heme oxygenase-1 expression in SH-SY5Y cells. Cell Biochem Funct. 2010;28(3):197–201.

55. Piao MJ, Kim KC, Choi J-Y, Choi J, Hyun JW. Silver nanoparticles down-regulate Nrf2-mediated 8-oxoguanine DNA glycosylase 1 through inactivation of extracellular regulated kinase and protein kinase B in human Chang liver cells. Toxicol Lett. 2011;207(2):143–148.

56. Kang SJ, Ryoo I-g, Lee YJ, Kwak M-K. Role of the Nrf2-heme oxygenase-1 pathway in silver nanoparticle-mediated cytotoxicity. Toxicol Appl Pharmacol. 2012;258(1):89–98.

APPENDIX

LIST OF ABBREVIATIONS

AgNPs	Silver nanoparticles
Bcl2	B-cell lymphoma 2
DMEM	Dulbecco's Modified Eagle Medium
EPO	Erythropoietin
FBS	Fetal bovine serum
FITC	Fluorescein isothiocyanate
GEPO	Glutaraldehyde erythropoietin
H2DCFDA	2', 7'-dichlofluorescein-diacetate
HEK293	Immortal human embryonic kidney cell line
JNK	c-Jun N-terminal kinase
Nrf2	Nuclear factor (erythroid-derived 2)-like 2
PBS	Phosphate buffered saline
PI3k/Akt	Phosphoinositide 3-kinase/Protein kinase B
PI	propidium iodide
PVDF	Polyvinylidene difluoride
ROS	Reactive oxygen species
TEM	Transmission electron microscope

EQUIPMENT AND CHEMICALS

1. Autoclave (Hirayama, Japan)
2. Biohazard Laminar Flow (Gibco, USA)
3. CO2 incubator (Esco, Singapore)
4. Laboratory balance (Denver instrument, Germany)
5. Microcentrifuge (Hettich, Germany)
6. pH meter (Denver instrument, Germany)
7. Phase contrast inverted microscope (Nikon, Japan
8. Transmission Electron Microscope (Hitachi, Japan)
9. Varioskan Flash microplate reader (Thermo, England)
10. Vortex mixer (Scientific industries, USA)
11. Water bath (Memmert, Germany)
12. 24-well plate (Corning, USA)
13. 96-well plate (Corning, USA)
14. Cell culture flask (SPL, Korea)
15. Centrifuge tube 1.5 mL (Corning, USA)
16. Centrifuge tube 15 mL (Corning, USA)
17. Centrifuge tube 50 mL (Corning, USA)
18. Dulbecco's Modified Eagle's Medium (Sigma, USA)
19. Fetal Bovine Serum (Gibco, USA)
20. Filter Tip (Corning, USA)
21. H2DCFDA (Molecular probes, USA)
22. Penicillin/Streptomycin (Gibco, USA)

23. PrestoBlue™ Cell viability Reagent (Invitrogen, USA)
24. Go Taq Flexi DNA polymerase (Promega, USA)
25. 25 bp DNA Ladder (Invitrogen, USA)
26. BSA (New England Biolabs, UK)
27. ACRYL/BIS 19:1 (ameresco, USA)
28. Ammonium persulfate (ameresco, USA)
29. TMET (Sigma-Aldrich, USA)

CHEMICAL PREPARATIONS

1. Phosphate buffer saline

KCl	0.2	g
KH2PO4	0.2	g
NaCl	8.0	g
Na2HPO4	1.15	g

Mix all of chemical components and add DI water to 1,000 mL, then adjust pH to 7.4 with HCl

2. Dulbecco's Modified Eagle's Medium (DMEM)

DMEM	13.4	g	(1 bottle)
Na2HCO3	3.7	g	
Fetal Bovine Serum	10%		
Pen/strep	1%		

Dissolve 13.4 g of DMEM and 3.7 g of Na2HCO3 with 800 mL DI water, then adjust pH to 7.2 with HCl and add DI water to 1,000 mL. Filtrate by 0.2 µM filter and keep as a stock medium. For working medium preparation, add 100 mL of Fetal Bovine Serum and 10 mL of antibiotic (Pen-Strep) into 890 mL of stock medium.

3. 10X TBE

Boric acid	27.5	g
Trist-base	54	g
0.5M EDTA (pH 8.0)	20	ml

4. 10x Running buffer

Tris-HCl (MW 121.14)	30.28 g
Glycine (MW 75.07)	144.13 g
Sodium dodecylsulfate (SDS)	10 g
Add dH2O up to 1000 ml	Store at 4ºc

5. 10x Transfer buffer

Tris-base (MW 121.14)	30.28 g
Glycine (MW 75.07)	144.13 g
Add ddH2O 800 ml	Store at 4ºc